



HAL
open science

What can gross alpha/beta activities tell about ^{210}Po and ^{210}Pb in the atmosphere?

Luca Terray, Donato D Amico, Olivier Masson, Jean-Christophe Sabroux

► To cite this version:

Luca Terray, Donato D Amico, Olivier Masson, Jean-Christophe Sabroux. What can gross alpha/beta activities tell about ^{210}Po and ^{210}Pb in the atmosphere?. *Journal of Environmental Radioactivity*, 2020, 255, pp.106437. 10.1016/j.jenvrad.2020.106437 . hal-03221235

HAL Id: hal-03221235

<https://hal.science/hal-03221235v1>

Submitted on 7 May 2021

HAL is a multi-disciplinary open access archive for the deposit and dissemination of scientific research documents, whether they are published or not. The documents may come from teaching and research institutions in France or abroad, or from public or private research centers.

L'archive ouverte pluridisciplinaire **HAL**, est destinée au dépôt et à la diffusion de documents scientifiques de niveau recherche, publiés ou non, émanant des établissements d'enseignement et de recherche français ou étrangers, des laboratoires publics ou privés.



Distributed under a Creative Commons Attribution - NonCommercial - NoDerivatives 4.0 International License

1 **Journal of Environmental Radioactivity**

2 **What can gross alpha/beta activities tell about ^{210}Po and ^{210}Pb in**
3 **the atmosphere?**

4 **Luca Terray** : *Laboratoire Magmas et Volcans, Université Clermont Auvergne,*
5 *Aubière, France Et Laboratoire de Physique de Clermont, Université Clermont*
6 *Auvergne, Aubière, France*

7 **Donato D'Amico, Olivier Masson et Jean-Christophe Sabroux** : *Institut de*
8 *Radioprotection et de Sûreté Nucléaire (IRSN), Fontenay-aux-Roses, France*

9

10 **What can gross alpha/beta activities tell about ^{210}Po and ^{210}Pb in the atmosphere?**

11 **Abstract:** ^{210}Po and ^{210}Pb represent the most abundant part of atmospheric aerosol long-
12 lived natural radioactivity. Moreover, ^{210}Pb - ^{210}Po monitoring in the atmosphere can be of
13 interest for tracking extreme natural events that can enhance the level of alpha/beta
14 radioactivity in air. In this paper, we question the possibility to use routine gross alpha/beta
15 measurements in order to monitor ^{210}Po , ^{210}Pb and $^{210}\text{Po}/^{210}\text{Pb}$ ratio in the atmosphere.
16 Based on joint gross alpha/beta measurement and ^{210}Pb - ^{210}Po specific determination on 16
17 atmosphere samples, we show that (i) gross beta activity systematically overestimates ^{210}Pb
18 activity due to the presence of interfering beta emitters and (ii) gross alpha activity mostly
19 reflects ^{210}Po activity even if an underestimation is always observed due to alpha particle
20 attenuation. In order to determine $^{210}\text{Po}/^{210}\text{Pb}$ ratio, we discuss the advantages of using
21 gross alpha activity time variation compared to specific ^{210}Po measurements. Finally, the
22 gross alpha/beta ratio appear to be a good proxy of the $^{210}\text{Po}/^{210}\text{Pb}$ ratio when large-scale
23 variations are to be monitored. We report a first reference level for the activity level of
24 airborne ^{210}Po in France of $13 \pm 6 \mu\text{Bq}/\text{m}^3$.

25

26

27

28

29

30

31

32 **1. Introduction**

33 Long-lived radon daughters (namely ^{210}Pb , ^{210}Bi and ^{210}Po) are widely used in
34 atmospheric studies (see recent reviews by Baskaran, 2011, 2016). These radionuclides can
35 be considered as tracers, as well as chronometers of air mass circulation. They are also
36 useful to determine the residence time and the removal rate of aerosols in the atmosphere.
37 In addition, they play a major role in the monitoring of atmospheric radioactivity because
38 they are responsible for the most part of long-lived (> 5 days) natural radioactivity of
39 atmospheric aerosols (see figure 1 and compilation in "Sources and effects of ionizing
40 radiation", UNSCEAR 2008 Report, 2010). Therefore, the levels of long-lived radon daughters
41 and their natural variability mostly influence reference levels and alert thresholds in the
42 atmospheric radioactivity monitoring and early warning context.

43 Extreme natural events such as volcanic eruptions, forest fires or dust resuspension events
44 are known to release important quantities of radioactive ^{210}Po into the atmosphere (*e.g.*
45 Lambert et al., 1982; Le Cloarec et al., 1995; Nho et al., 1996). For instance, Allard et al.
46 (2016) recently reported that Ambrym volcano (Vanuatu) is continuously emitting ^{210}Po into
47 the atmosphere at a rate of 210 TBq/year. In comparison, the estimated amount of
48 polonium released during the October, 1957 Windscale accident is 42 TBq (Garland and
49 Wakeford, 2007), which is to say only a fifth of the Ambrym cumulative emission in one year.
50 Moreover, such natural discharge episodes are likely to happen regularly and in many places
51 worldwide due to the important number of sources (either active volcanoes, burning
52 biomass or deserts), thus potentially increasing the exposure of local population to ionizing
53 radiations (^{210}Po is highly toxic when inhaled or ingested due to its very high specific activity

54 and emission of energetic alpha particles inside the body) and triggering anomalies of long-
55 lived alpha radioactivity in the atmosphere.

56 Consequently, it appears important for atmospheric radioactivity monitoring purposes
57 (including nuclear forensics) to be able to detect such events, which implies to discriminate
58 between natural and anthropogenic sources, and to assess the average background
59 concentration of airborne ^{210}Po .

60 In this article, we investigate the possibility of determining atmospheric $^{210}\text{Po}/^{210}\text{Pb}$ ratio
61 using gross alpha-beta activity measurements. Actually, both volcanic and forest fire plumes
62 are traced at long-distance by an increase in the $^{210}\text{Po}/^{210}\text{Pb}$ ratio compared to background
63 atmospheric values (Nho et al., 1997; Paatero et al., 2009). Indeed, high temperature
64 natural processes favour the release of the more volatile element, polonium, as compared to
65 lead. Thus, $^{210}\text{Po}/^{210}\text{Pb}$ ratio is a relevant clue to attribute an increase of atmospheric
66 radioactivity to an extreme natural event such as a volcanic eruption or a forest fire.

67 However, the specific measurement of ^{210}Po and ^{210}Pb at environmental levels requires
68 either a long analysis on a very sensitive Germanium detector (^{210}Pb) or a long and
69 destructive chemical process (^{210}Po) prior to radioactive counting. Therefore, a routine
70 monitoring of ^{210}Pb and ^{210}Po of atmospheric aerosols requires an important technical
71 support and is not easy to set up and maintain from the operational point of view.

72 Contrastingly, gross alpha/beta activity measurements are easier to perform on a regular
73 basis. Even if alpha/beta counting instruments are only able to discriminate beta and alpha
74 particles and do not allow to infer the nature of the radionuclide, the technique has strong
75 advantages: first, it does not need any sample preparation (the filter can be directly placed
76 inside the counter) and second, alpha/beta counting devices can generally host many

77 samples. For these two reasons, this technique is widely used in the field of aerosol
78 radioactivity monitoring. As far as France is concerned, there is a very dense network of
79 nuclear power plants and other nuclear installations in France monitoring gross alpha/beta
80 air indices on a daily basis (this network is referred to as *Réseau National de Mesures de la*
81 *radioactivité de l'environnement*, see the RNM website in the references). Therefore, if
82 alpha/beta gross activity ratio is found to be well representative of the $^{210}\text{Po}/^{210}\text{Pb}$ ratio it
83 would then be possible to track the signature of extreme or at least unusual natural events
84 with a simple (and already widely operational) routine procedure.

85 On one hand, the correlation between ^{210}Pb and beta long-lived (>5 days) activities in
86 atmospheric aerosol samples has already been evidenced (Mattsson et al., 1996) suggesting
87 that ^{210}Pb is responsible for most of the beta long-lived activity. Nevertheless, the presence
88 of other beta emitters (like ^{40}K , ^{32}P or ^{33}P) in the atmosphere is well known (Lal and Suess,
89 1968; Lujanien et al., 1997; Schery, 2001; Hernández et al., 2005) and can occasionally reach
90 significant levels. Occurrence of positive anomalies of these beta emitters could depend on
91 several factors (such as the locality of the sampling point and the history of the air mass) and
92 we still have to understand precisely the conditions leading to significant gaps between ^{210}Pb
93 and beta activity. On the other hand, the correlation between ^{210}Po and alpha activity has
94 never been clearly established (as far as we know) on an important series of samples. Even if
95 many individual measurements of the most naturally abundant alpha-emitters (^{238}U , ^{232}Th ,
96 ^{226}Ra) systematically point negligible activities compared to ^{210}Po , the outstanding
97 contributor of the alpha atmospheric radioactivity (see figure 1 and table 14 in "Sources and
98 effects of ionizing radiation", UNSCEAR 2008 Report,"2010), the validity of the
99 supposed correlation between ^{210}Po and gross alpha activities still needs to be evaluated.

100 In this study we collected a series of atmospheric aerosol samples and measured on the
101 same aliquot (see methods hereafter) ^{210}Pb , ^{210}Po and gross alpha/beta activities in order to
102 examine jointly the two aforementioned correlations. This allows us to finally assess the
103 constraints on $^{210}\text{Po}/^{210}\text{Pb}$ ratio provided by gross alpha/beta activity ratio.

104

105 **2. Methods**

106 **2.1 Atmospheric sampling**

107 Atmospheric aerosols have been sampled on the top of the building of the
108 Observatoire de Physique du Globe de Clermont-Ferrand (OPGC) located in the Campus des
109 Cézeaux (Aubière city, France) in the neighbourhood of Clermont-Ferrand city at an
110 elevation of about 400 m. We used a MegaVol-3000 particulate air sampler from Ecotech
111 that was operated at a flow rate of $150\text{ m}^3/\text{h}$. Air was pumped through a polypropylene filter
112 (3M) similar to the filters of OPERA-AIR network (see OPERA network website in the
113 references) with a minimum collection efficiency of about 95% for particles with an
114 aerodynamic diameter of 30 nm. The impacted area on the filter is a rectangle of 18 by 23
115 cm (414 cm^2).

116 Eleven samples were collected on a weekly basis between March and June 2017. Five more
117 samples were collected between February and June 2018. Sampling durations range
118 between 45 and 87 hours with a mean of 56 h, which is equivalent to a filtered air volume of
119 $8,400\text{ m}^3$. Starting time and sampling duration were decided in order to avoid important
120 precipitation events and shifts of meteorological regimes during sampling.

121 Each filter was dried and weighted before and after sampling in order to measure the
122 sampled mass of dry particulate matter. Sample details are provided in table 1.

123 2.2 Radioactivity analysis

124 Immediately after drying and weighting operations, a circular aliquot of 125 mm
125 diameter was cut in the centre of the filter and sent to IRSN-SAME laboratories in Le Vésinet,
126 France, for a set of analyses. SAME (Service d'Analyses et de Métrologie de l'Environnement)
127 is the service of IRSN in charge of environmental radioactivity measurements. The following
128 3-steps protocol was applied to the first eleven samples (collected in 2017):

- 129 - **Step 1:** gross alpha/beta counting of the aliquot and ^{210}Pb measurement by
130 gamma spectrometry (with a germanium detector) as soon as it was received,
131 approximately 5-10 days after sampling in order to get rid of the short-lived
132 radon and thoron daughters (see figure 1). These analyses will be referred to as
133 the 5-day analyses hereafter for convenience, even if some of them were not
134 exactly performed 5 days after sampling (see table 1). 5-day gross alpha/beta
135 counting is a typical measurement for most of atmospheric radioactivity
136 monitoring systems and such measurements are commonly available in many
137 places in France through a common sharing platform (see RNM website in the
138 references).
- 139 - **Step 2:** Repetition of step 1 (gross alpha/beta counting and gamma spectrometry
140 of the aliquot) 50 days after sampling, in order to reach the radioactive
141 equilibrium between ^{210}Bi and ^{210}Pb (^{210}Bi is the daughter of ^{210}Pb and has a half-
142 life of 5.2 days as compared to the 22.2-year half-life of its parent). These
143 analyses will be referred to as the 50-day analyses in the following. Such delayed
144 analyses are rarely performed in the context of aerosol radioactivity monitoring
145 but they present a significant interest when performed in addition to the 5-day

146 analyses. Indeed, this second set of measurements allows to make a direct
147 comparison between ^{210}Pb and gross beta activity. Actually, ^{210}Pb can only be
148 indirectly measured by the alpha/beta counter through the decay of its daughter
149 ^{210}Bi because the beta end-point energies of ^{210}Pb are too low (i.e. $E_{\text{max}}=17$ and 63
150 keV) to produce detectable electrons, while ^{210}Bi has a much higher beta end-
151 point energy ($E_{\text{max}} = 1162$ keV). After 50 days, ^{210}Bi activity is equal to ^{210}Pb
152 activity and then any difference between gross beta activity and ^{210}Pb activity is
153 necessarily due to other radionuclides present in the filter.

154 - **Step 3:** specific measurement of ^{210}Po by alpha spectrometry after mineralization
155 of the aliquot, chemical separation of polonium and plating of polonium onto
156 silver plates.

157 The same aliquot was systematically used for all analyses in order to avoid potential biases
158 due to sample heterogeneity. For the five samples collected in 2018, the protocol was
159 composed of steps 1 and 3, and step 3 started just after step 1 was completed in order to
160 minimize ^{210}Po build-up in the sample before the measurement by alpha spectrometry.

161 2.3 Meaning of gross alpha/beta activities

162 Detection yields of gross alpha/beta counting detectors have been determined using
163 ^{90}Sr - ^{90}Y sources for beta and ^{239}Pu for alpha. These sources have been produced by droplet
164 deposition of radioactive standard liquid solutions on blank filters. The type and geometry
165 of these filters were similar to those of samples in order to minimize calibration biases due
166 to different geometries and matrices between calibration sources and measured filters.
167 Accordingly, gross beta activity is expressed as equivalent ^{90}Sr activity and gross alpha
168 activity is expressed as equivalent ^{239}Pu activity.

169 However, since different radionuclides emit particles (either beta electrons or alpha
170 particles) with different energies, the detection yield obtained with some radionuclides (^{90}Sr -
171 ^{90}Y and ^{239}Pu in our case) might not be representative of the detection yield for any other
172 radionuclide. In order to better interpret the results, some qualitative considerations can be
173 made. As far as gross alpha activity is concerned, it should be noted that ^{239}Pu alpha particle
174 energies (5,105-5,156 keV) are close to ^{210}Po alpha particle energy (5,304 keV). Therefore,
175 the <4% relative difference of initial alpha particle energy might have a negligible effect on
176 the detection yield since it is similar or even lower compared to typical alpha energy
177 resolution measured above air filters (full width at half maximum from a few hundred keV
178 up to 1 MeV according to Moore et al., 1993). However, mechanisms affecting alpha activity
179 measurements of air filters are numerous and complex to assess (*e.g.* Geryes et al., 2009)
180 and a bias on the yield could still arise from external factors such as the depth of
181 radionuclide entrapment in the filter, or alpha energy absorption by aerosol particles
182 accumulated in and on the filter.

183 Contrastingly, gross beta activity might rather underestimate the activity of most beta
184 natural emitters such as ^{210}Bi , ^{40}K , ^{33}P , or ^{35}S . This is because beta electrons from a ^{90}Sr - ^{90}Y
185 mix have higher energies (561.4 keV on average) compared to beta electrons coming from
186 ^{210}Bi , ^{40}K , ^{33}P , or ^{35}S (317, 508.32, 76.4, and 48.79 keV on average, respectively). On the
187 contrary, ^{32}P emits beta electron with a mean energy of 695.5 keV and its activity could be
188 overestimated by the gross beta activity. However, this approach based on average beta
189 electron energy cannot be used for making quantitative bias assessments since it does not
190 take into account the geometry of the sample-detector ensemble and the shapes of energy
191 spectra at low energy where most of yield differences are rooted.

192 2.4 Correction of ^{210}Po build-up in the filter

193 Since ^{210}Pb has a 22.2 years half-life, it can be considered as stable during the whole
194 sampling and analysis periods. This is not the case for ^{210}Po due to its much shorter half-life
195 of only 138.4 days. Because the time lag between sampling and ^{210}Po analysis (typically 50-
196 70 days) is not negligible compared to ^{210}Po half-life, and because of the presence of ^{210}Pb
197 and ^{210}Bi in the filter, ^{210}Po can be regenerated (or eventually decay in the case of initial
198 $^{210}\text{Po}/^{210}\text{Pb}$ activity ratio greater than 1) in between the sampling time and the
199 measurement time . Thus, a correction has to be applied in order to infer the activity of the
200 filter at a given initial time prior to ^{210}Po measurement (either sampling time, 5-day or 50-
201 day analyses times). Since ^{210}Po can be regenerated in the filter by the decay of his parent
202 ^{210}Bi , itself sustained by the decay of ^{210}Pb , the correction depends on ^{210}Pb , ^{210}Bi and ^{210}Po
203 initial activities. The correction formula is given in appendix A. If necessary, the unknown
204 ^{210}Bi activity can be neglected (see appendix A).

205 2.5 Volume normalisation.

206 Atmospheric activities are finally calculated from the activities measured on the aliquot
207 (and subsequently corrected for ^{210}Po build-up), dividing by the volume of filtered air and
208 the aliquot to filter surface ratio (this ratio is similar for all samples and is equal to 0.3). It is
209 assumed that the analysed aliquot is representative of the whole filter.

210 2.6 Determination of $^{210}\text{Po}/^{210}\text{Pb}$ activity ratio from gross alpha activity time variation

211 Two different approaches can be used to determine the $^{210}\text{Po}/^{210}\text{Pb}$ activity ratio. The
212 first method simply consists in dividing ^{210}Po activity by ^{210}Pb activity. It is independent from
213 gross alpha/beta measurements but it implies a correction for ^{210}Po (see section 2.4). Since
214 this correction relies on the value of ^{210}Pb activity determined by gamma spectrometry with

215 high uncertainty owing to low counting statistics, the corrected ^{210}Po activity value at
216 sampling time can be affected by important errors. An alternative method relies on the
217 relative variation of gross alpha activity between 5-day and 50-day analyses and is based on
218 the hypothesis that this variation is only related to ^{210}Po variation inside the sample. This
219 assumption will be discussed later in the light of obtained results. The correction formula is
220 detailed in Appendix B.

221

222 **3. Results**

223 All measured atmospheric activities are reported in table 1 and plotted in figure 2. The
224 uncertainty is given at a significance level of 2 sigma (95%) and only includes the uncertainty
225 of the radioactivity measurements. Uncertainties on air volume and aliquot to filter ratio are
226 small compared to the uncertainty due to counting statistics and calibration, and are thus
227 neglected. What is more, errors related to the filtered volume or the aliquot to whole filter
228 ratio do not propagate an error on activity ratios.

229 3.1 Gross alpha/beta and ^{210}Pb activity levels

230 Gross alpha activity at 5 days was found at a level of $0.016 \pm 0.008 \text{ mBq/m}^3$ (mean and
231 standard deviation), and gross beta activity at 5 days was found at a level of 0.4 ± 0.2
232 mBq/m^3 (mean and standard deviation). These levels are consistent with the values usually
233 reported in the RNM. ^{210}Pb activity was found at a level of $0.3 \pm 0.2 \text{ mBq/m}^3$, which is in
234 good agreement with monthly averages previously recorded at sites located nearby our
235 sampling site by Bourcier et al. (2011), *i.e.*, from $0.33 \pm 0.10 \text{ mBq/m}^3$ to $1.13 \pm 0.34 \text{ mBq/m}^3$
236 at the Opme station (5.7 km SSW from our sampling site), and from $0.34 \pm 0.04 \text{ mBq/m}^3$ to
237 $1.35 \pm 0.14 \text{ mBq/m}^3$ at the Puy-de-Dôme observatory.

238 3.2 Gross beta activity versus ^{210}Pb activity at 5 and 50 days and the excess of gross beta
239 activity

240 Figure 3 displays 5-day beta activities as a function of ^{210}Pb activities. A marked
241 correlation between these two activities is found ($R^2=0.98$), but ^{210}Pb activity is significantly
242 lower than beta activity ($\beta = 1.27 \times ^{210}\text{Pb} + 0.05 \text{ mBq/m}^3$, best fit). At 50 days, a marked
243 correlation between gross beta and ^{210}Pb activities is also found ($\beta = 1.44 \times ^{210}\text{Pb} - 0.02$
244 mBq/m^3 , $R^2 = 0.97$). These excellent correlations at 5 and 50 days mean that ^{210}Bi coming
245 from ^{210}Pb decay is the main source of long-lived beta radioactivity of atmospheric aerosols
246 (*i.e.*, still present in the filter 5 days after sampling), in good agreement with previous studies
247 (*e.g.*, Mattsson et al., 1996). However, obtained linear coefficients are significantly higher
248 than 1 meaning that gross beta activity is in excess compared to ^{210}Pb activity. As stated
249 previously, gross beta activity might underestimate ^{210}Bi activity and therefore this excess
250 cannot be due to a calibration bias (if such a bias exists). At 5 days, ^{210}Bi activity could be
251 higher than ^{210}Pb activity but this possibility can likely be discarded since $^{210}\text{Bi}/^{210}\text{Pb}$ activity
252 ratio is generally < 1 in tropospheric air with a typical value of 0.5 (Poet et al., 1972).
253 Moreover, at 50 days, when ^{210}Pb and ^{210}Bi are in radioactive equilibrium, the clear
254 discrepancy observed between gross beta and ^{210}Pb activities proves that long-lived
255 radionuclides different from ^{210}Pb contribute to gross beta activity. Assuming that calibration
256 biases can be neglected, it is thus possible to calculate the amount of beta radioactivity
257 coming from those other sources. We find that the mean excess beta activity compared to
258 ^{210}Pb - ^{210}Bi equilibrium activity is 0.1 mBq/m^3 (with a standard deviation of $\pm 0.1 \text{ mBq/m}^3$).
259 Could such an excess be explained by the presence of other beta emitters like ^{40}K , ^{32}P , ^{33}P , or
260 ^{35}S ? ^{40}K activity was not detected by gamma spectrometry for any sample in this study and
261 detection thresholds were typically higher than 0.1 mBq/m^3 ($1.4 \pm 0.7 \text{ mBq/m}^3$, mean and

262 standard deviation of detection thresholds). However, ^{40}K activity levels measured at the
263 nearby Opme station (5.7 km SSW from our sampling site) (OPERA-AIR network) in the
264 period March 2017-June 2018 are significantly lower than 0.1 mBq/m^3 with an average value
265 of $6.2 \pm 3.2 \text{ } \mu\text{Bq/m}^3$ (Olivier Masson, unpublished data). Even if some episodic events with
266 high ^{40}K atmospheric activities (Hernández et al., 2005) cannot be ruled out, these low-level
267 measurements suggest that ^{40}K cannot be the main beta emitter contributing to the
268 observed excess. ^{32}P , ^{33}P , and ^{35}S are pure beta emitters and therefore they cannot be
269 measured by gamma spectrometry. However, the order of magnitude of airborne activity
270 levels reported in the literature for ^{32}P , ^{33}P and ^{35}S (Lal and Suess, 1968; Lujanien et al., 1997)
271 is about 0.1 mBq/m^3 . When summed up, the activities of cosmogenic radionuclides might
272 exceed the observed excess of beta activity ($\sim 0.1 \text{ mBq/m}^3$). Nevertheless, the beta detection
273 yield of ^{33}P and ^{35}S with a gross alpha/beta counting device might be very small due the low
274 energy of electrons emitted by these nuclides (see section 2.3) and therefore only a minor
275 part of their activity is accounted for in the measured gross beta activity. Thus, we suggest
276 that the observed beta excess is compatible with a contribution of cosmogenic
277 radionuclides.

278 3.3 Inferences on the gross beta activity excess from comparison between 5 and 50 days

279 Figure 4a represents gross beta activity at 5 and 50 days, as well as ^{210}Pb activity, for
280 each of the 2017 samples. It can be observed that gross beta activity at 5 days is
281 systematically higher than or similar to gross beta activity at 50 days. This observation is a
282 further argument in favour of the contribution of cosmogenic radionuclides to the gross beta
283 activity. Indeed, all the above-cited radionuclides have half-lives of a few tens of days: 14.3
284 days (^{32}P), 25.4 days (^{33}P) and 87.3 days (^{35}S). Therefore, their activity in the filter
285 significantly decreases between 5 and 50 days.

286 In order to check whether the decrease of ^{32}P , ^{33}P and ^{35}S is compatible with the observed
287 decrease of gross beta activity, it is possible to calculate the apparent half-life of the gross
288 beta activity excess (relative to ^{210}Pb) using the following equation:

$$\tau_{app} = \frac{-\Delta t \ln 2}{\ln \frac{\beta_{50} - ^{210}\text{Pb}}{\beta_5 - ^{210}\text{Pb}}}$$

289 (eq. 1)

290 where Δt corresponds to the interval between 5-day and 50-day analyses and β and ^{210}Pb
291 correspond to gross beta activity and ^{210}Pb activity, respectively. This calculation is
292 illustrated on figure 4b. Values of τ_{app} calculated for the ten samples acquired in 2017 range
293 from 30 to 1500 days with a median value of 80 days and mean value of 271 days (one
294 sample with lower gross beta activity at 5 days as compared to 50 days was excluded). Half
295 of the computed values are higher than the expected half-lives. However, τ_{app} must be
296 considered as a maximum estimate of the beta excess half-life since the increase in ^{210}Bi
297 activity between 5 and 50 days could partially counter-balance the activity decrease of short-
298 lived cosmogenic radionuclides. Indeed, ^{210}Bi activity is generally lower than ^{210}Pb in the
299 troposphere (see above), therefore the activity of ^{210}Bi in the filter gradually increases until
300 radioactive equilibrium is reached with ^{210}Pb after about one month.

301 Actually, two groups of samples can tentatively be separated: a six-sample group with a low
302 apparent half-life (from 30 to 80 days, mean 50 days) associated to a significant gross beta
303 activity decrease and a four-sample group with a high apparent half-life (from 160 to 1560
304 days, mean 680 days) corresponding with a barely significant decrease or lack of significant
305 decrease. The first group might be composed of samples with higher ^{32}P - ^{33}P - $^{35}\text{S}/^{210}\text{Pb}$ activity
306 ratios and/or a $^{210}\text{Bi}/^{210}\text{Pb}$ initial activity ratio closer to 1 (smaller ^{210}Bi build-up).

307 Alternatively, the second group 2 can be composed of samples with lower ^{32}P - ^{33}P - $^{35}\text{S}/^{210}\text{Pb}$
308 activity ratios and/or lower $^{210}\text{Bi}/^{210}\text{Pb}$ initial activity ratio (higher ^{210}Bi build-up).

309

310 3.4 Gross alpha activity versus ^{210}Po activity at 50 days

311 Figure 5 compares 50-day gross alpha activity and ^{210}Po activity. Reported polonium
312 activities are corrected for the build-up taking place between the gross alpha/beta counting
313 at 50 days and ^{210}Po measurement 10 to 20 days after (see methods for more details).

314 Uncertainties are calculated by quadratic propagation of ^{210}Po measurement uncertainty
315 and ^{210}Pb activity uncertainty (used for the correction, see appendix A). An excellent linear
316 correlation between the two activities is found ($R^2 = 0.99$) and gross alpha activity at 50 days
317 is lower than ^{210}Po activity (best fit: $\alpha = 0.83 \times ^{210}\text{Po}$ mBq/m³, mean ratio of 0.72). Linear
318 correlation between the two activities strongly suggests that ^{210}Po is the main source of
319 alpha activity at 50 days. This is in agreement with previously reported activity levels of only
320 0.5-1 $\mu\text{Bq}/\text{m}^3$ for long-lived alpha emitters in the atmosphere (^{238}U , ^{230}Th , ^{226}Ra , ^{232}Th , ^{228}Ra ,
321 ^{228}Th) ("Sources and effects of ionizing radiation", UNSCEAR 2008 Report, 2010 and
322 references therein). The fact that alpha gross alpha activity is smaller than ^{210}Po activity can
323 be explained by the measurement process and alpha particles self-absorption in the filter
324 (see discussion).

325 3.5 Gross alpha activity at 5 days versus build-up corrected ^{210}Po activity

326 Figure 6a represents gross alpha activity measured at 5 days as a function of build-up
327 corrected 5-day ^{210}Po activity (see methods). In marked contrast with the situation at 50
328 days, gross alpha and ^{210}Po activities are poorly correlated ($R^2 = 0.77$ for 2017 samples and
329 $R^2 = 0.78$ for 2018 samples), even though positive correlation trends are still observed.

330 Interestingly, even if correlation coefficients are similarly low for 2017 and 2018, the 2018
331 samples group (characterized by a shorter time lag before ^{210}Po measurement) present a
332 mean alpha/ ^{210}Po ratio closer to the mean ratio found for 50-day activities (5-day ratios of
333 0.66 for 2018 samples and 0.4 for 2017 samples, to be compared to the 50-day ratio of 0.72).
334 Moreover, the uncertainty on build-up corrected ^{210}Po activity is much higher for the 2017
335 sample group than for the 2018 sample group (see figure 6a). Since the 5-day alpha/ ^{210}Po
336 ratio has no obvious reason to change between 2017 and 2018 and since ^{210}Po is the
337 outstanding contributor of long-lived alpha radioactivity (see figure 1), these observations
338 suggest that the correction applied to ^{210}Po activity in order to recalculate its value backward
339 in time introduces an important dispersion and bias in the corrected values, especially when
340 the correction lag is long (2017 sample group). Therefore, obtained ^{210}Po corrected activities
341 cannot be trusted as representative of ^{210}Po atmospheric level for 2017 samples.
342 Contrastingly, the good agreement between 5-day alpha/ ^{210}Po ratio of 2018 samples and the
343 50-day ratio suggests that corrected ^{210}Po activities are not significantly biased.

344 3.6 Atmospheric $^{210}\text{Po}/^{210}\text{Pb}$ activity ratio inferred from gross alpha activity variation 345 (2017 samples)

346 Due to large uncertainty propagation on corrected ^{210}Po activity using the ^{210}Pb -
347 based approach (see section 3.5), we attempted to determine $^{210}\text{Po}/^{210}\text{Pb}$ activity ratio using
348 the gross alpha activity variation method described in section 2.6. Results are presented in
349 figure 7. This method relies on the assumption that the relative increase of gross alpha
350 activity between 5 and 50 days is equal to the relative increase of ^{210}Po activity in the filter.
351 Conclusions drawn from section 3.4 confirm that long-lived alpha-emitting radionuclides
352 found in the atmosphere (U, Th and Ra isotopes) are not active enough to invalid this

353 assumption (see also figure 1). Another source of uncertainty behind this method is the lack
354 of constraints on $^{210}\text{Bi}/^{210}\text{Pb}$ activity ratio in the filter. In order to evaluate the effect the
355 unknown $^{210}\text{Bi}/^{210}\text{Pb}$ activity ratio on this method, $^{210}\text{Po}/^{210}\text{Pb}$ activity ratio is calculated for
356 three different values of this parameter in equation B.4 (appendix B), i.e. 0, 0.5 and 1.

357 It is clear on figure 7 that the value of $^{210}\text{Bi}/^{210}\text{Pb}$ initial activity ratio has an effect on the
358 value of $^{210}\text{Po}/^{210}\text{Pb}$ activity ratio obtained from gross alpha activity variation (the higher the
359 assumed $^{210}\text{Bi}/^{210}\text{Pb}$ ratio, the lower the obtained initial $^{210}\text{Po}/^{210}\text{Pb}$ ratio). However, taking
360 into account uncertainties of gross alpha activity measurements, the results obtained with
361 different values of the $^{210}\text{Bi}/^{210}\text{Pb}$ ratio are not significantly different. Therefore, the effect of
362 ^{210}Bi can be neglected and we will consider afterward a mean value of 0.5 for $^{210}\text{Bi}/^{210}\text{Pb}$
363 ratio (Poet et al., 1972).

364 First, the obtained $^{210}\text{Po}/^{210}\text{Pb}$ ratio (0.07 ± 0.01 , mean and standard deviation) is very close
365 to the 5-day gross alpha/ ^{210}Pb activity ratio (0.06 ± 0.02). In comparison, the $^{210}\text{Po}/^{210}\text{Pb}$
366 mean ratio obtained from build-up corrected ^{210}Po activity is 0.18 ± 0.07 . This shows that the
367 gross alpha activity variation method causes lower biases as compared to the ^{210}Po build-up
368 correction. Moreover, $^{210}\text{Po}/^{210}\text{Pb}$ activity ratios obtained with this method are in good
369 agreement with the mean atmospheric value of 0.06 previously reported by Daish et al.
370 (2005).

371 Using the same method, we computed the 5-day $^{210}\text{Po}/^{210}\text{Pb}$ ratio for each sample (taking
372 into account the exact time lag between sampling and 5-days analysis) and derived the 5-day
373 ^{210}Po activity (multiplying by ^{210}Pb activity) that we compared to 5-day gross alpha activity
374 (figure 6b). A much better correlation is found as compared to that of the other method ($R^2 =$
375 0.95 versus 0.77). Moreover, the 5-day alpha/ ^{210}Po ratio obtained with the gross alpha

376 activity variation method is in good agreement with the alpha/ ^{210}Po ratio found at 50 days.
377 These results confirm that the alpha/ ^{210}Po ratio might not significantly change between 5
378 days and 50 days, and demonstrates that ^{210}Po is the dominant long-lived alpha emitter of
379 atmospheric aerosols.

380

381 3.7 Atmospheric $^{210}\text{Po}/^{210}\text{Pb}$ activity ratio versus gross alpha/beta activity ratio

382 Figure 8 represents gross alpha/beta activity ratio measured at 5 days as a function of
383 atmospheric $^{210}\text{Po}/^{210}\text{Pb}$ activity ratio inferred from gross alpha activity variation (2017
384 samples) and from corrected ^{210}Po activity (2018 samples). The two activity ratios are not
385 well correlated ($R^2 = 0.12$ and 0.46 for 2017 and 2018 respectively). Gross alpha/beta activity
386 ratio is lower than $^{210}\text{Po}/^{210}\text{Pb}$ activity ratio by a mean factor of 0.9 (2017) or 0.6 (2018).
387 Lower alpha/beta activity ratio as compared to $^{210}\text{Po}/^{210}\text{Pb}$ activity ratio is logical since 5-day
388 gross beta activity overestimates ^{210}Pb activity (see section 3.2) and since alpha activity
389 underestimate ^{210}Po activity (see section 3.4). Thus, both differences tend to an
390 underestimation of $^{210}\text{Po}/^{210}\text{Pb}$ activity ratio by the alpha/beta activity ratio. However, it
391 should be pointed out that both ratios are almost always compatible considering the large
392 error bars, especially for the $^{210}\text{Po}/^{210}\text{Pb}$ activity ratio. Actually, gross alpha/beta activity
393 ratio has a typical relative uncertainty of $22\% \pm 14\%$ ($k=2$) while $^{210}\text{Po}/^{210}\text{Pb}$ ratios present
394 larger relative uncertainties ($36\% \pm 2\%$ in 2018 and $50\% \pm 20\%$ in 2017). For both kinds of
395 ratio, the relative variability of the sample set (2σ standard deviation divided by mean) is not
396 considerably higher than measurement uncertainties (48% for alpha/beta ratio and 70% for
397 $^{210}\text{Po}/^{210}\text{Pb}$ ratio).

398 3.8 ^{210}Po levels in France

399 Based on the estimate of atmospheric $^{210}\text{Po}/^{210}\text{Pb}$ activity ratio and on measured ^{210}Pb
400 activities, it is possible to determine the airborne ^{210}Po activity level at the study site. We
401 find a level of ^{210}Po of $13 \pm 6 \mu\text{Bq}/\text{m}^3$ (mean and standard deviation on all samples). This
402 level is in very good agreement with levels reported in England by Daish et al., 2005 ($12,3 \pm$
403 $0,4 \mu\text{Bq}/\text{m}^3$) and constitutes the first chronicle of ^{210}Po activity in France.

404

405 **4. Discussion**

406 4.1 Origin and consequences of the gross beta activity excess compared to ^{210}Pb

407 Gross beta activity is found in marked excess as compared to ^{210}Pb activity by a typical
408 factor of ~ 1.3 (see section 3.2). This excess is higher at 5 days than at 50 days after sampling
409 and can be attributed to the presence of short-lived cosmogenic radionuclides (see sections
410 3.2 and 3.3). This factor can serve as a correction factor to retrieve ^{210}Pb activity from 5-day
411 gross beta activity. However, it is interesting to point out that a previous comparison study
412 (based on a larger set of samples) did not identify this phenomenon (Mattsson et al., 1996).
413 The authors found a regression equation equivalent to $\beta = 1.03 \times ^{210}\text{Pb} + 0.02 \text{ mBq}/\text{m}^3$ (see
414 figure 9 in Mattsson et al., 1996) even if some samples could present a beta excess factor as
415 large as 1.3. Even if a calibration bias cannot be ruled out, we suggest that the typical beta
416 activity excess compared to ^{210}Pb (and the correction factor to apply) may depend on the
417 location and on the potential presence of local sources of other beta emitters. As a
418 consequence, the use of gross beta activity to infer ^{210}Pb activity might be cautious and
419 requires a calibration of gross beta activity vs ^{210}Pb to be made on site, for instance using the
420 protocol presented in this study. If such a calibration of gross beta activity vs ^{210}Pb activity

421 was performed on a large number of sampling stations, it would be possible to understand
422 how the excess of gross beta activity relates to environmental conditions.

423 In this study, the two gross beta activity has been measured only two times for each sample
424 (at 5 and 50 days). Yet, we have shown that gross beta activity likely reflects the presence of
425 several short-lived radionuclides including ^{210}Pb - ^{210}Bi , ^{32}P , ^{33}P and ^{35}S . Thus, we suggest that
426 precise constraints on the nature of the beta excess could be obtained with at least 5 gross
427 beta activity measurements over a period of 50 days.

428 4.2 Alpha particles self-absorption in filters

429 The gross alpha activity has been found to slightly underestimate ^{210}Po activity when
430 both activities are compared at 50 days. The cause of this difference likely lies in the
431 measurement process itself. Actually, measurement of alpha emitters in air filters is known
432 to be strongly biased by alpha particles attenuation inside aerosol particles and filter media
433 (Geryes et al., 2009 and references therein). Alpha particles interact efficiently with aerosol
434 particles and filter fibers and can possibly be stopped before reaching the detector which
435 causes a decrease in the gross detection efficiency. The correction of the alpha attenuation
436 in air filter consists in calibrating the alpha/beta counting apparatus with a filter
437 impregnated with a known amount of alpha radioactivity (see section 2.3). However, the
438 attenuation endured by alpha particles in the calibration filter can be slightly different from
439 the attenuation occurring in real atmospheric air filters. This could be explained, for
440 instance, because of different mechanisms of fixation (water droplets percolation versus
441 aerosols fixation) or because of attenuation caused by aerosol particles themselves. This
442 difference could result in a biased calibration coefficient. In the present case, we suggest
443 that alpha attenuation is slightly underestimated resulting in an underestimate of the gross

444 alpha activities by approximately 10% (see section 3.4). Therefore, in the context of
445 atmospheric radioactivity monitoring we recommend to calibrate alpha counting devices
446 using real aerosol filters in order to avoid potential matrix biases. The reference value of
447 alpha activity for calibration filters can be obtained via radiochemistry, as presented in this
448 study.

449

450 4.3 Advantages and disadvantages of ^{210}Po measurement strategies in atmospheric 451 samples

452 Since ^{210}Po is regenerated in the samples by ^{210}Pb and ^{210}Bi decays, precise measurement
453 of this radionuclide in the atmosphere is challenging. If ^{210}Po is not measured within a few
454 days at most after sampling, its activity significantly increases in the sample which implies to
455 make a correction to retrieve the original ^{210}Po content. Yet, this correction depends on
456 ^{210}Pb which is difficult to estimate directly with high precision (since it requires long counting
457 times). Therefore, important errors can be made on the initial ^{210}Po activity due to error
458 propagation and amplification from ^{210}Pb measurement. Moreover, ^{210}Bi activity is also
459 needed in the correction process, as variable $^{210}\text{Bi}/^{210}\text{Pb}$ initial activity ratios will affect the
460 build-up of ^{210}Po by ^{210}Pb decay. This problem has also been investigated by Lozano et al.
461 (2011). Yet, precise measurement of ^{210}Bi is also challenging since it is a pure beta emitter
462 mixed with other beta emitters in the filter. Its quantification would require either a
463 chemical separation or a continuous measurement of beta activity over a few weeks in order
464 to perform the proper deconvolution of the half-lives of the different beta emitters present
465 in the filter (^{33}P , ^{32}P , ^{35}S , ^{40}K , ^{210}Bi).

466 It has been shown that ^{210}Po activity values corrected for build-up by ^{210}Bi - ^{210}Pb decay in the
467 filter in between 5 and 50 days are largely biased due to error propagation (see 3.5). This is
468 not surprising since this correction relies on ^{210}Pb activity measured by gamma spectrometry
469 with high uncertainty (typical relative uncertainty of 30% in our study) and since any error on
470 ^{210}Pb activity propagates to ^{210}Po activity. Contrastingly, the same correction formula was
471 used for recalculating ^{210}Po activity at 50 days (typical correction of 10-20 days, see table 1)
472 and did not introduce any notable dispersion (see section 3.4). The same observation stands
473 true for 2018 samples for which the time lag between 5-day alpha/beta counting and ^{210}Po
474 measurement was 24 days at most . This suggests that the dispersion induced by the
475 correction is amplified as ^{210}Po activity is recalculated sooner backward in time. Therefore,
476 precise ^{210}Po specific activity determination implies a short time lag between sampling and
477 analysis (typically 10-20 days). If this condition is met, this technique has the major
478 advantage of being direct.

479 Another ^{210}Po measurement strategy is based on $^{210}\text{Po}/^{210}\text{Pb}$ ratio determination using gross
480 alpha activity variation with time. Compared to direct determination of ^{210}Po , this method
481 has the main advantage to be simpler (no radiochemistry is needed). It is also worth to point
482 out that this method is not affected by alpha particle attenuation bias since it is based on the
483 relative increase of gross alpha activity. However, the waiting period to obtain the result is
484 longer since two gross alpha activity measurements are required, at 5 and 50 days, in order
485 to determine the initial $^{210}\text{Po}/^{210}\text{Pb}$ ratio. What is more, this method is based on the
486 assumption that the relative increase of gross alpha activity is equal to the ^{210}Po true relative
487 increase in the filter. Potential reasons for rejecting this assumption would be the presence
488 of other alpha emitters in the filter. Regarding long-lived radionuclides, the comparison at 50
489 days between gross alpha activity and ^{210}Po activity demonstrates that no contribution can

490 be detected since an excellent correlation is found between the two activities. However,
491 short-lived radionuclides with significant initial activity compared to ^{210}Po could have
492 completely decayed and could be missed at 50 days. Such radionuclides would likely have a
493 half-life shorter than ~ 10 days. Conversely, they must have a half-life $> \sim 1$ day to be still
494 active in the sample at 5 days (this is not the case for all radon and thoron daughters). A
495 search in a radionuclide database indicates that potential candidates for naturally occurring
496 alpha-emitters with a half-life between 1 and 10 days are ^{223}Ra and ^{224}Ra . For both nuclides,
497 we found no atmospheric activity reported in the literature. However, airborne ^{228}Th (^{224}Ra
498 father in the ^{232}Th decay chain) activity has occasionally been reported to be about $1 \mu\text{Bq}/\text{m}^3$
499 (Kolb, 1989). Therefore we suggest that ^{224}Ra activity level is in the same order of magnitude
500 due its short half-life (3.6 days). Such level is very low compared to the amplitude of gross
501 alpha activity variation (tens of $\mu\text{Bq}/\text{m}^3$) and would not affect the final result. Because ^{223}Ra
502 originates from the ^{235}U decay chain, which is much less abundant than ^{232}Th and ^{238}U in
503 nature (0.7% of uranium and $\text{Th}/\text{U} = 4.2$), we suggest that ^{223}Ra levels in the atmosphere are
504 likely to be even lower than ^{224}Ra levels. Therefore, it appears that the initial assumption
505 lying behind the method is robust.

506 When compared in term of final result uncertainty, the gross alpha activity variation method
507 is more reliable than direct ^{210}Po determination if the time lag between sampling and ^{210}Po
508 determination is long (typically 50-70 days). Conversely, if the time lag is short (10-20 days)
509 the two methods give similar results, even if the typical relative uncertainty is higher for the
510 gross alpha activity variation method as compared to direct ^{210}Po determination (50%
511 compared to 35%). Since both methods are based on measured ^{210}Pb activity, it should
512 finally be noted that the uncertainty of both methods would decrease if a more precise ^{210}Pb
513 activity measurement is available.

514 4.4 Alpha/beta activity ratio versus $^{210}\text{Po}/^{210}\text{Pb}$ activity ratio and the detection of
515 extreme natural events

516 5-day alpha and beta activities are routinely measured in many locations for
517 monitoring reasons. Thus, large databases of alpha/beta activity ratio are available and could
518 be used to study ^{210}Po and ^{210}Pb in the atmosphere. When comparing this ratio with our
519 estimates of $^{210}\text{Po}/^{210}\text{Pb}$ activity ratio, we found that both ratios match each other due to
520 large uncertainties. Due to the rather low number of samples (16) and to the fact that
521 $^{210}\text{Po}/^{210}\text{Pb}$ and gross alpha/beta ratio variability did not significantly exceed the
522 measurement uncertainty, it is not possible to conclude about the correlation between the
523 two ratios. However, when looking at mean ratios, our data suggest that alpha/beta activity
524 ratio is smaller than $^{210}\text{Po}/^{210}\text{Pb}$ activity ratio. This underestimation is potentially due to two
525 phenomena: (i) presence of other beta emitters leading to an overestimation of ^{210}Pb by
526 gross beta activity and (ii) calibration error on alpha measurement due to an inappropriate
527 treatment of alpha self-absorption in the filter, leading to underestimation of ^{210}Po by gross
528 alpha activity.

529 The amplitude of these two biases has been determined in sections 3.2, 3.4, 3.5 and 3.6.
530 Considering the mean and standard deviation of alpha/ ^{210}Po ratios (see figures 5 and 6a, b)
531 determined at 5 and 50 days with different methods, it is possible to infer a typical
532 alpha/ ^{210}Po ratio of 0.7 with a sample-to-sample variability of 15%. At 5 days, the beta/ ^{210}Pb
533 ratio has a mean value of 1.5 with a variability of 15%. Thus, it is possible to infer a typical
534 factor of 0.5 between gross alpha/beta and $^{210}\text{Po}/^{210}\text{Pb}$ activity ratios with a 1σ variability of
535 20%. Consequently, the gross alpha/beta activity ratio appears to be suitable for tracking
536 relative $^{210}\text{Po}/^{210}\text{Pb}$ ratio variations much larger than 20% (*i.e.* at least 100%). Yet, relative

537 variations of ^{210}Po activity associated with savanna fire plumes or volcanic plumes often
538 exceed this threshold as reported by several authors (e.g., Le Cloarec et al., 1995; Nho et al.,
539 1996, 1997). Therefore, the gross alpha/beta ratio might be able to record such variations.
540 Finally it is possible to imagine a protocol dedicated to the monitoring of these extreme
541 natural events:

- 542 - The protocol is triggered on when 5-day alpha/beta ratio is 100% larger than the
543 reference value.
- 544 - A gamma spectrometry is performed as long as possible to obtain ^{210}Pb activity in
545 the sample.
- 546 - If possible, an aliquot is analysed as soon as possible for ^{210}Po determination.
- 547 - In any case, several gross alpha/beta countings are performed during 50 days to
548 better constrain the initial $^{210}\text{Bi}/^{210}\text{Pb}$ and $^{210}\text{Po}/^{210}\text{Pb}$ ratios and the cosmogenic
549 radionuclides.

550

551 5. Conclusion

552 Gross alpha/beta activity and specific ^{210}Po and ^{210}Pb activity measurements have been
553 performed on a set of atmospheric aerosols samples in order to investigate co-variations of
554 these different activities. Several main conclusions can be drawn:

- 555 - Beta activity was found to systematically overestimate ^{210}Pb activity by ~30%.
556 Using 5 and 50-day gross beta activity measurements, it is possible to constrain
557 the nature of this beta activity excess. We show that it is mostly due to short-
558 lived beta emitters (^{33}P , ^{32}P , and ^{35}S).

559

- 560 - 50-day gross alpha activity is mainly due to ^{210}Po . However, alpha activity is found
561 to underestimate ^{210}Po activity. This is likely due to the alpha energy attenuation
562 in the filter that is difficult to properly take into account in the calibration
563 process.
- 564
- 565 - Determination of ^{210}Po activity in the atmosphere from delayed ^{210}Po
566 measurement (from 15 to 90 days after sampling in this study) is very challenging
567 due to the effect of ^{210}Po build-up from ^{210}Pb and ^{210}Bi decay. We show that the
568 uncertainty increases as the timespan of correction increases and that the
569 corrected value can be significantly biased.
- 570
- 571 - However, indirect estimation of $^{210}\text{Po}/^{210}\text{Pb}$ activity ratio can be obtained from
572 gross alpha activity variation between 5 and 50 days. Mean $^{210}\text{Po}/^{210}\text{Pb}$ activity
573 ratio obtained using this method is in very good agreement with alpha/ ^{210}Pb
574 activity ratio, meaning that the method is not strongly biased although it is
575 indirect.
- 576
- 577 - alpha/beta activity ratio tend to underestimate $^{210}\text{Po}/^{210}\text{Pb}$ activity ratios due to
578 discrepancies between gross beta and ^{210}Pb activities (presence of other beta
579 emitters), on one hand, and between gross alpha and ^{210}Po activities on the other
580 hand (alpha particle attenuation). However, large-scale $^{210}\text{Po}/^{210}\text{Pb}$ ratio
581 variations typical of extreme natural events could still be monitored through
582 gross alpha/beta measurements.
- 583

584 - A first estimation of atmospheric ^{210}Po activity level in France is $13 \pm 6 \mu\text{Bq}/\text{m}^3$.

585

586

587 **APPENDIX A: correction of ^{210}Po build-up in the filter.**

588 ^{210}Po activity measured at a given time t must be corrected to take into account the
 589 build-up of this radionuclide by ^{210}Bi decay in the sample. The formula of this correction can
 590 be obtained by solving the decay equations for a three-member chain ($1 \rightarrow 2 \rightarrow 3$, or
 591 $^{210}\text{Pb} \rightarrow ^{210}\text{Bi} \rightarrow ^{210}\text{Po}$). To do so we use the formalism of Bateman given by Pressyanov (2002)
 592 where radionuclide initial numbers are factorized and we transform it to express the
 593 solution with activities instead of numbers:

$$594 \quad A_i(t) = A_{i,0} e^{-\lambda_i t} + \sum_{m=1}^{i-1} A_{m,0} \prod_{q=m+1}^i \lambda_q \sum_{k=m}^i \frac{e^{-\lambda_k t}}{\prod_{j=m}^i (\lambda_j - \lambda_k)}$$

595 (eq. A.1)

596 where $A_i(t)$ stands for the activity of the i -th nuclide in the decay chain, $A_{i,0}(t)$ for the initial
 597 activity of i (at $t = 0$), λ_i for the decay constant of i and t for the time. In the case of $^{210}\text{Pb} \rightarrow$
 598 $^{210}\text{Bi} \rightarrow ^{210}\text{Po}$ ($1 \rightarrow 2 \rightarrow 3$) decay chain, the equation A.1 translates to:

$$(Po)_t = (Po)_0 C_{Po}^t + (Bi)_0 C_{Bi}^t + (Pb)_0 C_{Pb}^t$$

599 (eq. A.2)

600 where $(X)_0$ is the activity of the aliquot at a given initial time and $(X)_t$ is the activity of the
 601 same aliquot after a time t (X corresponding either with ^{210}Pb , ^{210}Bi or ^{210}Po , the 210
 602 exponent is not reproduced in the equation for simplicity). C_X^t is a numerical coefficient that
 603 is a function of time t and of radioactive decay constants of ^{210}Pb , ^{210}Bi and ^{210}Po :

$$C_{Po}^t = e^{-\lambda_{Po} t}$$

$$C_{Bi}^t = \frac{\lambda_{Po}}{\lambda_{Po} - \lambda_{Bi}} e^{-\lambda_{Bi} t} + \frac{\lambda_{Po}}{\lambda_{Bi} - \lambda_{Po}} e^{-\lambda_{Po} t}$$

$$C_{Pb}^t = \frac{\lambda_{Po}\lambda_{Bi}}{(\lambda_{Po} - \lambda_{Pb})(\lambda_{Bi} - \lambda_{Pb})} e^{-\lambda_{Pb}t} + \frac{\lambda_{Po}\lambda_{Bi}}{(\lambda_{Po} - \lambda_{Bi})(\lambda_{Pb} - \lambda_{Bi})} e^{-\lambda_{Bi}t} + \frac{\lambda_{Po}\lambda_{Bi}}{(\lambda_{Bi} - \lambda_{Po})(\lambda_{Pb} - \lambda_{Po})} e^{-\lambda_{Po}t}$$

604 (eqs. A.3, A.4 & A.5)

605 Using this formalism it is possible to infer initial polonium content of the sample using the
606 following equation:

$$(Po)_0 = \frac{(Po)_t - (Bi)_0 C_{Bi}^t - (Pb)_0 C_{Pb}^t}{C_{Po}^t}$$

607 (eq. A.6)

608 In the right member of equation A.6, $(Po)_t$ is measured, $(Pb)_0$ is constant through short
609 times and is determined by gamma spectrometry and C_{Bi}^t , C_{Pb}^t and C_{Po}^t are directly
610 calculated from t . Only $(Bi)_0$ is not directly measured. When ^{210}Po activity is to be
611 recalculated at 50-day analysis time, $(Bi)_0$ is equal to $(Pb)_0$ because of radioactive
612 equilibrium and equation A.6 simplifies. When ^{210}Po activity is to be recalculated at sampling
613 time, or at 5 days, it is not possible to assume radioactive equilibrium. However, it is possible
614 to show that the initial ^{210}Bi activity can be neglected. Let us rewrite equation A.6:

$$(Po)_0 = \frac{(Po)_t}{C_{Po}^t} - \frac{(Pb)_0 C_{Pb}^t}{C_{Po}^t} \left(1 + \frac{(Bi)_0 C_{Bi}^t}{(Pb)_0 C_{Pb}^t} \right)$$

615 (eq. A.7)

616 We can neglect the contribution of ^{210}Bi initial activity if it is smaller than the ^{210}Pb term
617 contribution, in other words if:

$$\frac{(Bi)_0 C_{Bi}^t}{(Pb)_0 C_{Pb}^t} \ll 1$$

618

(eq. A.8)

619 First, $C_{\text{Bi}}^t/C_{\text{Pb}}^t$ is about 10% for $t = 50$ days. Second, $^{210}\text{Bi}/^{210}\text{Pb}$ activity ratio of atmospheric
 620 aerosols is generally reported lower than 1 with a mean value of 0.5 (e.g. Poet et al., 1972).
 621 Therefore, it is likely that the contribution of the ^{210}Bi term in equation 4 is no more than 10
 622 % of the contribution of ^{210}Pb , and likely around 5 %. Because the typical uncertainty on
 623 ^{210}Pb values measured by gamma spectrometry is larger than 10 % (see table 1), it is
 624 legitimate to neglect ^{210}Bi initial activity in the correction formula. Equation A.7 can thus be
 625 simplified as:

$$(\text{Po})_0 = \frac{(\text{Po})_t - (\text{Pb})_0 C_{\text{Pb}}^t}{C_{\text{Po}}^t}$$

626

(eq. A.9)

627 Finally, the uncertainty of corrected ^{210}Po activity is obtained by convolution of the
 628 uncertainties of ^{210}Po and ^{210}Pb measurements:

$$u((\text{Po})_0) = \frac{1}{C_{\text{Po}}^t} \sqrt{u^2((\text{Po})_t) + u^2((\text{Pb})_0) C_{\text{Pb}}^t{}^2}$$

629

(eq. A.10)

630 where $u(v)$ stands for the uncertainty on the measured quantity v .

631

632

633

634

635 **Appendix B: determination of $^{210}\text{Po}/^{210}\text{Pb}$ activity ratio from gross alpha activity increase**
 636 **between 5 and 50 days.**

637 Supposing that gross alpha activity relative variation between 5 and 50 days is only
 638 due to ^{210}Po , we can write:

$$\frac{\alpha_{50} - \alpha_5}{\alpha_5} = \frac{(\text{Po})_{50} - (\text{Po})_5}{(\text{Po})_5}$$

639 (eq. B.1)

640 where α and $(\text{Po})_t$ correspond to gross alpha activity and ^{210}Po activity respectively (either
 641 at 5 or 50 days). Replacing right terms of equation B.1 by their expression given by equation
 642 A.2, the relative variation of gross alpha activity becomes:

$$\begin{aligned} \frac{\alpha_{50} - \alpha_5}{\alpha_5} &= \frac{(C_{\text{Pb}}^{50} - C_{\text{Pb}}^5)(\text{Pb})_0 + (C_{\text{Bi}}^{50} - C_{\text{Bi}}^5)(\text{Bi})_0 + (C_{\text{Po}}^{50} - C_{\text{Po}}^5)(\text{Po})_0}{C_{\text{Pb}}^5(\text{Pb})_0 + C_{\text{Bi}}^5(\text{Bi})_0 + C_{\text{Po}}^5(\text{Po})_0} \\ &= \frac{\Delta C_{\text{Pb}}(\text{Pb})_0 + \Delta C_{\text{Bi}}(\text{Bi})_0 + \Delta C_{\text{Po}}(\text{Po})_0}{C_{\text{Pb}}^5(\text{Pb})_0 + C_{\text{Bi}}^5(\text{Bi})_0 + C_{\text{Po}}^5(\text{Po})_0} \end{aligned}$$

643 (eq. B.2)

644 where $\Delta C_X = C_X^{50} - C_X^5$. Dividing by $(\text{Po})_0$ and using the notation R_0 for $^{210}\text{Po}/^{210}\text{Pb}$ initial
 645 activity ratio, equation B.2 becomes:

$$\frac{\alpha_{50} - \alpha_5}{\alpha_5} = \frac{\Delta C_{\text{Pb}}R_0^{-1} + \Delta C_{\text{Bi}}(\text{Bi}/\text{Pb})_0R_0^{-1} + \Delta C_{\text{Po}}}{C_{\text{Pb}}^5R_0^{-1} + C_{\text{Bi}}^5(\text{Bi}/\text{Pb})_0R_0^{-1} + C_{\text{Po}}^5}$$

646 (eq. B.3)

647 Noting $\delta = \frac{\alpha_{50} - \alpha_5}{\alpha_5}$ the relative variation of gross alpha activity, we can finally obtain an

648 expression of R_0 as a function of δ :

$$R_0 = \frac{C_{\text{Pb}}^5 \delta - \Delta C_{\text{Pb}} + \left(\frac{\text{Bi}}{\text{Pb}}\right)_0 (C_{\text{Bi}}^5 \delta - \Delta C_{\text{Bi}})}{\Delta C_{\text{Po}} - C_{\text{Po}}^5 \delta}$$

649

(eq. B.4).

650 Of course, this expression of $^{210}\text{Po}/^{210}\text{Pb}$ activity ratio depends also on the $^{210}\text{Bi}/^{210}\text{Pb}$ activity

651 ratio and can be simplified if an assumption on the $^{210}\text{Bi}/^{210}\text{Po}$ initial activity ratio is made.

652

653

654 **References**

- 655 Allard, P., Aiuppa, A., Bani, P., Métrich, N., Bertagnini, A., Gauthier, P.-J., Shinohara, H.,
 656 Sawyer, G., Parello, F., Bagnato, E., Pelletier, B., Garaebiti, E., 2016. Prodigious
 657 emission rates and magma degassing budget of major, trace and radioactive volatile
 658 species from Ambrym basaltic volcano, Vanuatu island Arc. *Journal of Volcanology
 659 and Geothermal Research, Understanding volcanoes in the Vanuatu arc* 322, 119–
 660 143. <https://doi.org/10.1016/j.jvolgeores.2015.10.004>
- 661 Baskaran, M., 2016. Applications of Radon Progeny in Atmospheric Studies, in: Baskaran, M.
 662 (Ed.), *Radon: A Tracer for Geological, Geophysical and Geochemical Studies*, Springer
 663 Geochemistry. Springer International Publishing, Cham, pp. 85–117.
 664 https://doi.org/10.1007/978-3-319-21329-3_5
- 665 Baskaran, M., 2011. Po-210 and Pb-210 as atmospheric tracers and global atmospheric Pb-
 666 210 fallout: a Review. *Journal of Environmental Radioactivity, International Topical
 667 Meeting on Polonium and Radioactive Lead Isotopes* 102, 500–513.
 668 <https://doi.org/10.1016/j.jenvrad.2010.10.007>
- 669 Bourcier, L., Masson, O., Laj, P., Pichon, J.M., Paulat, P., Freney, E., Sellegri, K., 2011.
 670 Comparative trends and seasonal variation of ⁷Be, ²¹⁰Pb and ¹³⁷Cs at two altitude
 671 sites in the central part of France. *Journal of Environmental Radioactivity* 102, 294–
 672 301. <https://doi.org/10.1016/j.jenvrad.2010.12.005>
- 673 Daish, S.R., Dale, A.A., Dale, C.J., May, R., Rowe, J.E., 2005. The temporal variations of ⁷Be,
 674 ²¹⁰Pb and ²¹⁰Po in air in England. *Journal of Environmental Radioactivity* 84, 457–
 675 467. <https://doi.org/10.1016/j.jenvrad.2005.05.003>
- 676 Garland, J.A., Wakeford, R., 2007. Atmospheric emissions from the Windscale accident of
 677 October 1957. *Atmospheric Environment* 41, 3904–3920.
 678 <https://doi.org/10.1016/j.atmosenv.2006.12.049>
- 679 Geryes, T., Monsanglant-Louvet, C., Gehin, E., 2009. Experimental and simulation methods
 680 to evaluate the alpha self-absorption factors for radioactive aerosol fiber filters.
 681 *Radiation Measurements, Proceedings of the 24th International Conference on
 682 Nuclear Tracks in Solids* 44, 763–765. <https://doi.org/10.1016/j.radmeas.2009.10.059>
- 683 Hernández, F., Hernández-Armas, J., Catalán, A., Fernández-Aldecoa, J.C., Karlsson, L., 2005.
 684 Gross alpha, gross beta activities and gamma emitting radionuclides composition of
 685 airborne particulate samples in an oceanic island. *Atmospheric Environment* 39,
 686 4057–4066. <https://doi.org/10.1016/j.atmosenv.2005.03.035>
- 687 Kolb, W., 1989. Seasonal fluctuations of the uranium and thorium contents of aerosols in
 688 ground-level air. *Journal of Environmental Radioactivity* 9, 61–75.
 689 [https://doi.org/10.1016/0265-931X\(89\)90038-6](https://doi.org/10.1016/0265-931X(89)90038-6)
- 690 Lal, D., Suess, H.E., 1968. The Radioactivity of the Atmosphere and Hydrosphere. *Annual
 691 Review of Nuclear Science* 18, 407–434.
 692 <https://doi.org/10.1146/annurev.ns.18.120168.002203>
- 693 Le Cloarec, M.F., Ardouin, B., Cachier, H., Liousse, C., Neveu, S., Nho, E.-Y., 1995. ²¹⁰Po in
 694 savanna burning plumes. *J Atmos Chem* 22, 111–122.
 695 <https://doi.org/10.1007/BF00708184>
- 696 Lozano, R.L., Miguel, E.G.S., Bolívar, J.P., 2011. Assessment of the influence of in situ ²¹⁰Bi in
 697 the calculation of in situ ²¹⁰Po in air aerosols: Implications on residence time
 698 calculations using ²¹⁰Po/²¹⁰Pb activity ratios. *Journal of Geophysical Research:
 699 Atmospheres* 116. <https://doi.org/10.1029/2010JD014915>

700 Lujanienė, G., Ogorodnikov, B.I., Budyka, A.K., Skitovich, V.I., Lujanas, V., 1997. An
701 investigation of changes in radionuclide carrier properties. *Journal of Environmental*
702 *Radioactivity* 35, 71–90. [https://doi.org/10.1016/S0265-931X\(96\)00014-8](https://doi.org/10.1016/S0265-931X(96)00014-8)
703 Mattsson, R., Paatero, J., Hatakka, J., 1996. Automatic Alpha/Beta Analyser for Air Filter
704 Samples - Absolute Determination of Radon Progeny by Pseudo-Coincidence
705 Techniques. *Radiat Prot Dosimetry* 63, 133–139.
706 <https://doi.org/10.1093/oxfordjournals.rpd.a031520>
707 Moore, M.E., McFarland, A.R., Rodgers, J.C., 1993. Factors That Affect Alpha Particle
708 Detection in Continuous Air Monitor Applications. *Health Physics* 65, 69–81.
709 Nho, E.-Y., Ardouin, B., Le Cloarec, M.F., Ramonet, M., 1996. Origins of ²¹⁰Po in the
710 atmosphere at Lamto, Ivory Coast: Biomass burning and Saharan dusts. *Atmospheric*
711 *Environment* 30, 3705–3714. [https://doi.org/10.1016/1352-2310\(96\)00093-3](https://doi.org/10.1016/1352-2310(96)00093-3)
712 Nho, E.-Y., Cloarec, M.-F.L., Ardouin, B., Ramonet, M., 1997. ²¹⁰Po, an atmospheric tracer of
713 long-range transport of volcanic plumes. *Tellus B: Chemical and Physical Meteorology*
714 49, 429–438. <https://doi.org/10.3402/tellusb.v49i4.15980>
715 OPERA network [WWW Document], n.d. URL [https://www.irsn.fr/en/research/scientific-](https://www.irsn.fr/en/research/scientific-tools/experimental-facilities-means/opera/Pages/Opera-network.aspx)
716 [tools/experimental-facilities-means/opera/Pages/Opera-network.aspx](https://www.irsn.fr/en/research/scientific-tools/experimental-facilities-means/opera/Pages/Opera-network.aspx) (accessed
717 6.17.20).
718 Paatero, J., Vesterbacka, K., Makkonen, U., Kyllönen, K., Hellen, H., Hatakka, J., Anttila, P.,
719 2009. Resuspension of radionuclides into the atmosphere due to forest fires. *Journal*
720 *of Radioanalytical and Nuclear Chemistry* 282, 473–476.
721 <https://doi.org/10.1007/s10967-009-0254-9>
722 Poet, S.E., Moore, H.E., Martell, E.A., 1972. Lead 210, bismuth 210, and polonium 210 in the
723 atmosphere: Accurate ratio measurement and application to aerosol residence time
724 determination. *Journal of Geophysical Research (1896-1977)* 77, 6515–6527.
725 <https://doi.org/10.1029/JC077i033p06515>
726 RNM [WWW Document], n.d. URL <https://www.mesure-radioactivite.fr/en#/expert>
727 (accessed 6.17.20).
728 Schery, S.D., 2001. *Understanding radioactive aerosols and their measurement*. Springer
729 Science & Business Media.
730 Sources and effects of ionizing radiation, UNSCEAR 2008 Report, 2010. . Volume I. Annex A.
731 United Nations, New York.
732

Figures and tables

Table 1: Sampling details and analysis results. All uncertainties are given with a coverage factor $k=2$. ^{210}Po activity is given at the time of ^{210}Po deposition onto plates. All activities are expressed in mBq/m^3 considering sampled volumes and a constant aliquot/filter surface ratio of 0.3.

Sample	Sampling start (local time)	Sampling duration (h)	Sampled volume (m^3)	Dust load ($\mu\text{g}/\text{m}^3$)	1st gross alpha/beta counting delay (d)	Gross activity 5 days (mBq/m^3)		2 nd gross alpha/beta counting delay (d)	Gross activity 50 days (mBq/m^3)		^{210}Pb activity (mBq/m^3)	^{210}Po meas. delay (d)	^{210}Po activity (mBq/m^3)
						alpha	beta		alpha	beta			
1	27/3/17 14:08	50,6	7582	3	7	0,011 ± 0,003	0,224 ± 0,009	63	0,038 ± 0,004	0,203 ± 0,009	0,18 ± 0,05	91	0,09 ± 0,01
2	4/4/17 11:33	73,8	11073	15	5	0,008 ± 0,002	0,203 ± 0,007	63	0,032 ± 0,003	0,178 ± 0,007	0,16 ± 0,04	82	0,055 ± 0,006
3	12/4/17 18:40	47,9	7181	15	11	0,017 ± 0,003	0,33 ± 0,01	56	0,055 ± 0,007	0,31 ± 0,02	0,21 ± 0,03	110	0,11 ± 0,01
4	14/4/17 18:35	87,0	13050	10	7	0,010 ± 0,002	0,257 ± 0,008	52	0,038 ± 0,003	0,224 ± 0,007	0,16 ± 0,02	71	0,067 ± 0,007
5	21/4/17 13:53	71,6	10742	10	10	0,020 ± 0,003	0,48 ± 0,01	56	0,069 ± 0,004	0,39 ± 0,01	0,30 ± 0,03	65	0,10 ± 0,01
6	2/5/17 12:54	45,9	6893	6	5	0,004 ± 0,003	0,180 ± 0,008	53	0,018 ± 0,003	0,138 ± 0,008	0,09 ± 0,02	82	0,045 ± 0,005
7	12/5/17 18:02	63,3	9485	5	4	0,007 ± 0,002	0,162 ± 0,007	56	0,025 ± 0,003	0,160 ± 0,007	0,10 ± 0,02	71	0,038 ± 0,005
8	23/5/17 13:45	51,9	7781	12	6	0,013 ± 0,003	0,39 ± 0,01	56	0,069 ± 0,005	0,39 ± 0,01	0,27 ± 0,03	69	0,10 ± 0,01
9	7/6/17 13:22	52,3	7843	12	7	0,008 ± 0,003	0,30 ± 0,01	56	0,035 ± 0,003	0,228 ± 0,009	0,19 ± 0,03	61	0,047 ± 0,005
10	13/6/17 11:49	52,3	7845	15	11	0,033 ± 0,003	0,77 ± 0,02	64	0,147 ± 0,007	0,75 ± 0,02	0,60 ± 0,05	69	0,19 ± 0,02
11	21/6/17 13:36	48,2	7228	23	6	0,035 ± 0,004	0,91 ± 0,02	112	0,30 ± 0,01	1,05 ± 0,03	0,68 ± 0,06	118	0,35 ± 0,04
12	26/2/18 15:45	49,1	7363	17	9	0,020 ± 0,003	0,47 ± 0,02				0,28 ± 0,08	15	0,034 ± 0,005
13	18/4/18 9:08	52,1	7825	23	7	0,020 ± 0,003	0,66 ± 0,02				0,45 ± 0,06	17	0,046 ± 0,007
14	20/6/18 9:05	49,9	7491	18	14	0,022 ± 0,004	0,45 ± 0,01				0,29 ± 0,03	20	0,036 ± 0,005
15	27/6/18 9:45	47,7	7138	17	17	0,020 ± 0,003	0,37 ± 0,01				0,22 ± 0,04	21	0,030 ± 0,003
16	21/9/18 16:14	64,3	9631	6	19	0,015 ± 0,002	0,248 ± 0,008				0,12 ± 0,03	24	0,021 ± 0,002

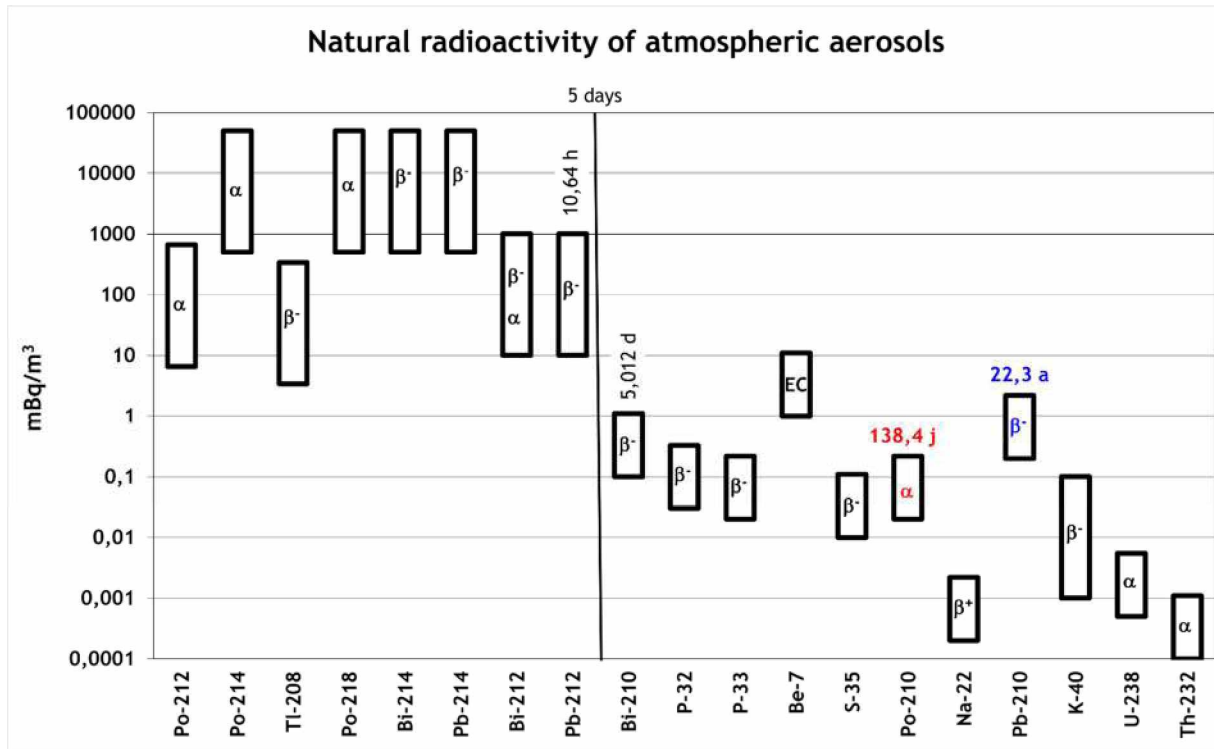


Figure 1: Repartition of the natural radioactivity of atmospheric aerosols. The main radionuclides are sorted on the x axis from short-period to long-period. The main decay mode (alpha, beta or electronic capture) is also indicated. Data are taken from the 2008 UNSCEAR report (Sources and effects of ionizing radiation, UNSCEAR 2008 Report, 2008) and from Schery (2001). All short-lived ^{222}Rn daughters have half-lives considerably smaller than 5 days. Contrastingly, most ^{220}Rn daughters (from the ^{232}Th chain) are part of the progeny of ^{212}Pb which has a 10.64 hours half-life. Therefore, the long-lived radioactivity can only be measured after 5 days when ^{212}Pb has thoroughly decayed out (5 days corresponds with eleven ^{212}Pb periods and a 2000 fold reduction of the initial activity). This long-lived radioactivity comes from three different types of radionuclides: long-lived ^{222}Rn daughters (^{210}Pb , ^{210}Bi , ^{210}Po), radionuclides of cosmogenic origin (^{32}P , ^{33}P , ^7Be , ^{35}S , ^{22}Na) and “primordial” radionuclides (^{40}K , ^{238}U , ^{232}Th) injected in the atmosphere upon soil erosion. Long-lived alpha activity is largely dominated by ^{210}Po . ^{210}Pb is the most active long-lived beta emitter but other radionuclides are also significant (^{32}P , ^{33}P , ^{35}S , ^{40}K).

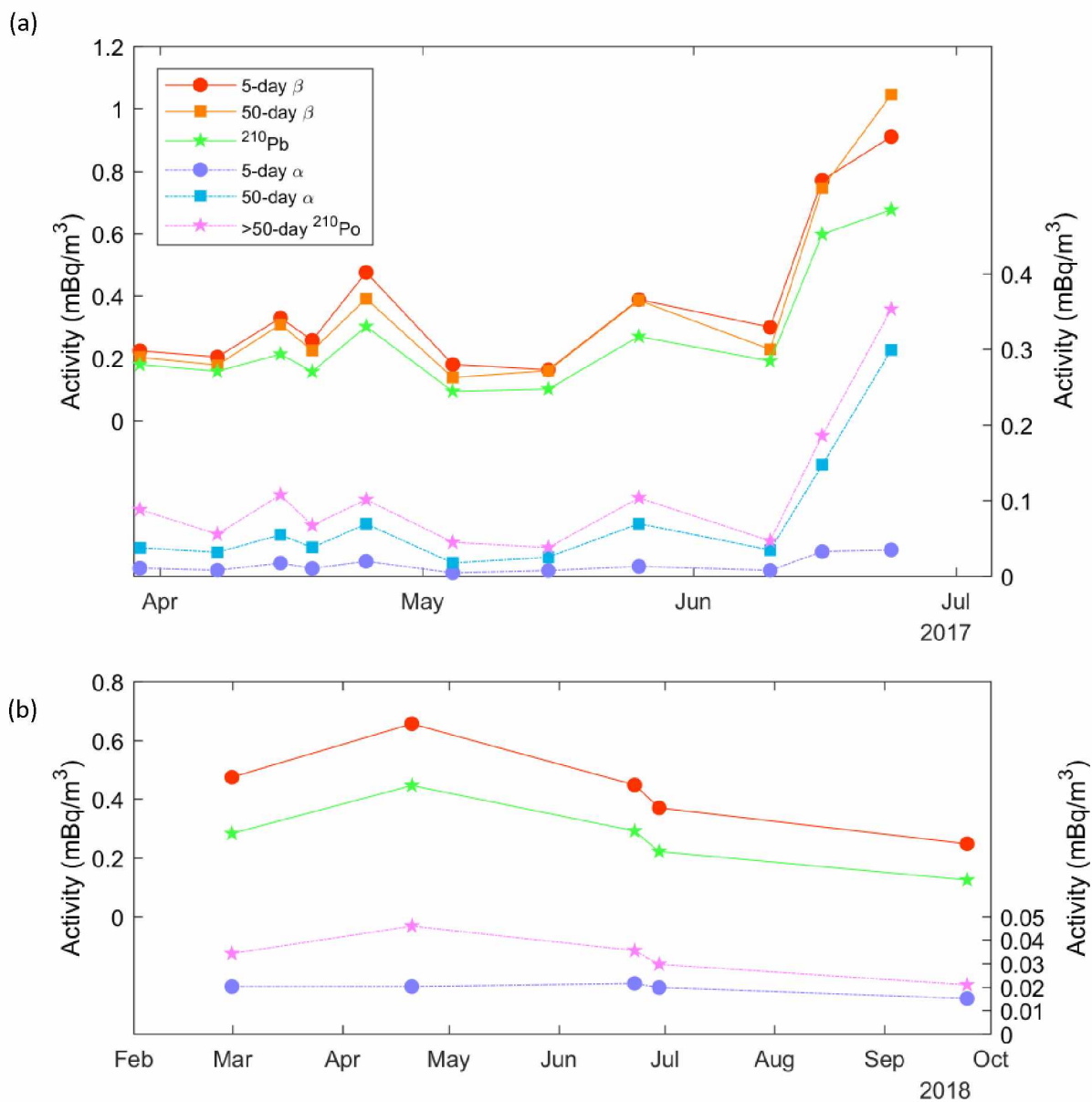


Figure 2: Activities recorded for all samples in 2017 (a) and 2018 (b), including 5 and 50-day gross alpha/beta activities, ²¹⁰Pb activity measured by gamma spectrometry and ²¹⁰Po activity measured by alpha spectrometry after chemical separation (activities reported on the graph are not corrected for ²¹⁰Po ingrowth between sampling and measurement). Error bars are not drawn to avoid visual overload but are provided in table 1.

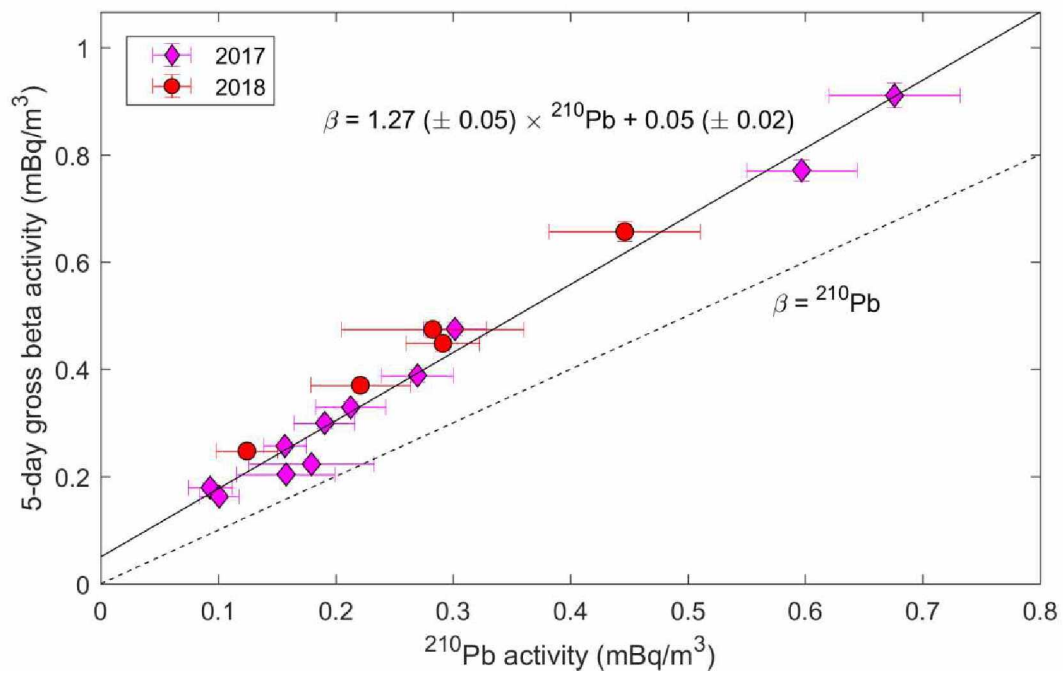


Figure 3: 5-day gross beta activity versus ^{210}Pb activity of all samples (2017 and 2018 sample groups). The best linear fit ($R^2 = 0.98$) and the $y=x$ line (dash line) are also plotted.

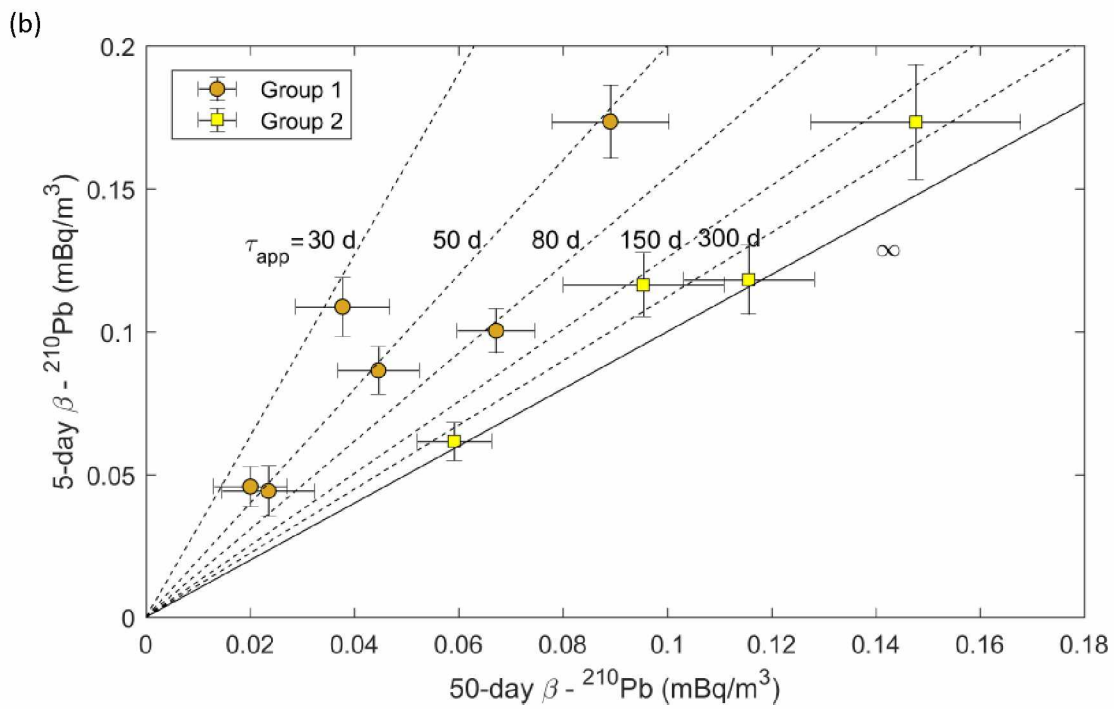
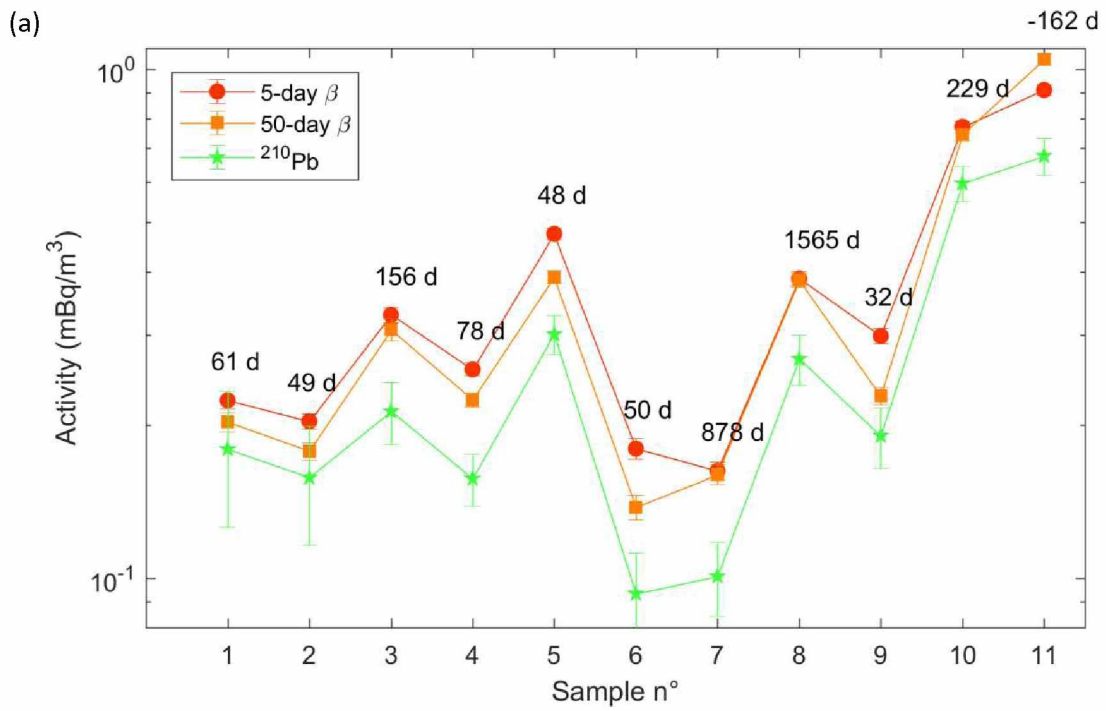


Figure 4: (a) 5-day and 50-day gross beta activities and ²¹⁰Pb activity for all 2017 samples with the corresponding computed half-life of un-sustained beta activity decay (see section 3.3 for details) in days.

(b) Excess of gross beta activity relative to ^{210}Pb activity at 5 days (y axis) and at 50 days (x axis). Error bars are calculated taking into account gross beta activity uncertainty only. Iso-lines of apparent half-life are also plotted for some values of the half-life (see section 3.3). Two groups are distinguished: group 1 for samples presenting significantly different 5 and 50-day gross beta activities at, group 2 for samples presenting similar 5 and 50-day gross beta activities.

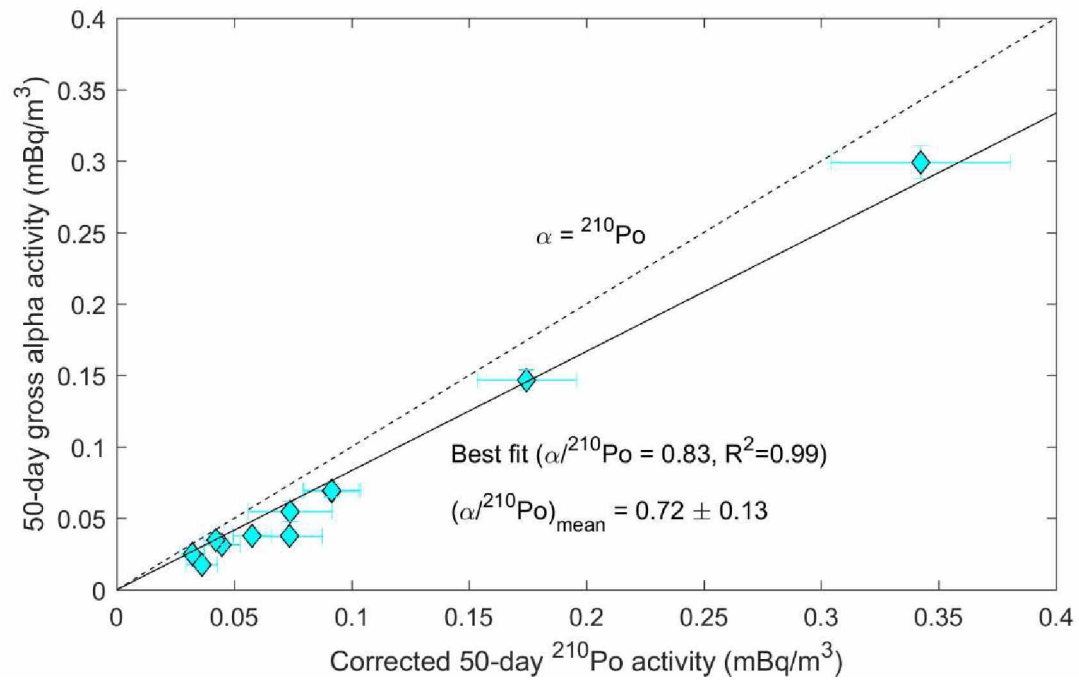


Figure 5: 50-day gross alpha activity versus ²¹⁰Po activity recalculated at 50 days (2017 sample group, see appendix A for calculation details). The best linear fit ($R^2 = 0.99$) and the $y=x$ line (dash line) are also plotted.

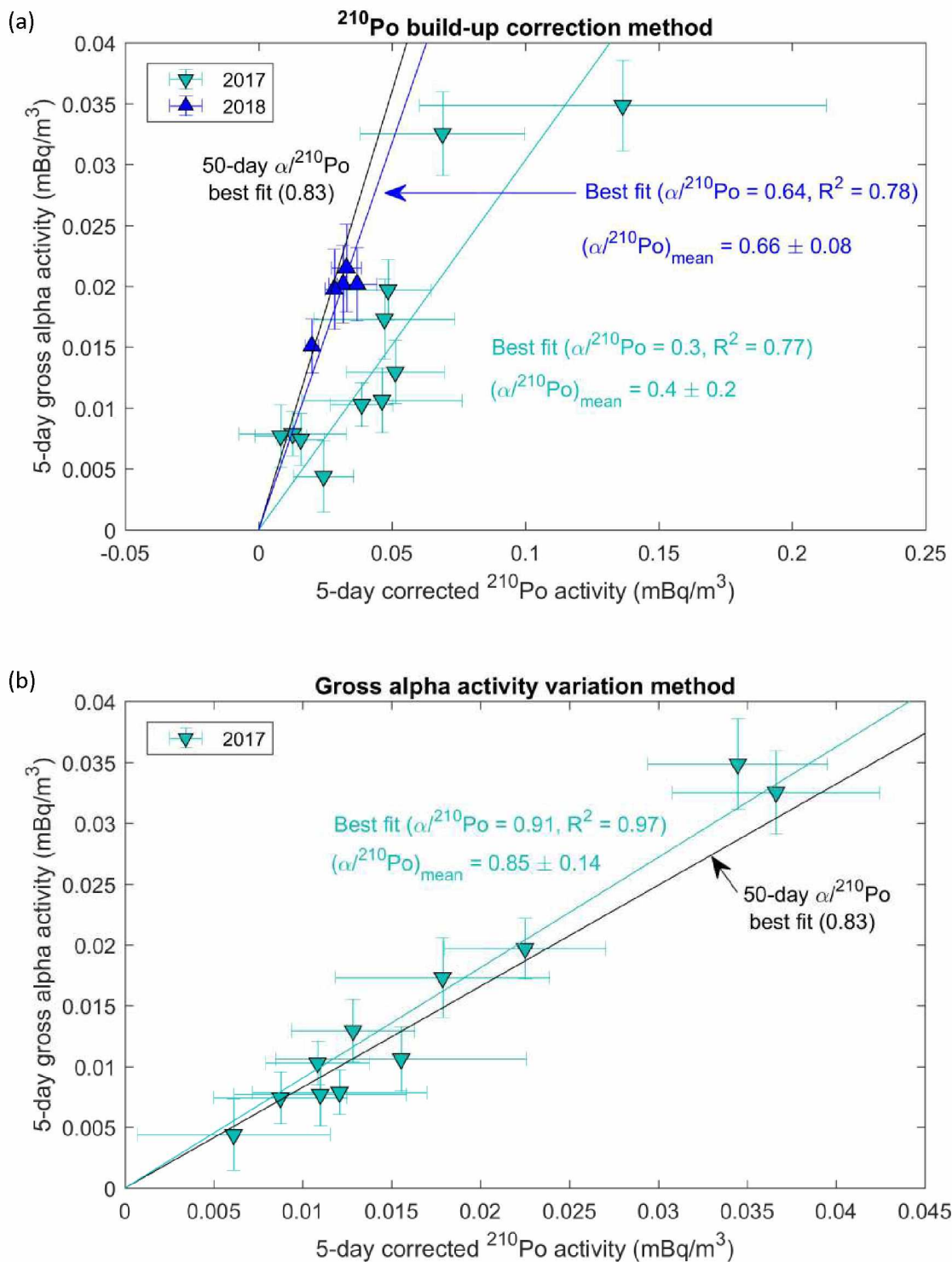


Figure 6: Correlation of 5-day gross alpha activity and ^{210}Po activity recalculated at $t = 5$ days using different approaches: (a) build-up correction of ^{210}Po activity (see appendix A for calculation details) and (b) determination of $^{210}\text{Po}/^{210}\text{Pb}$ activity ratio from gross alpha activity variation between 5 and 50 days (see appendix B for calculation details). For each

method, the mean alpha/²¹⁰Po activity ratio is plotted (coloured lines) and compared to the alpha/²¹⁰Po measured at 50 days (0.83, black line). All uncertainties are propagated to the corrected ²¹⁰Po activity. Moreover, mean and standard deviation of alpha/²¹⁰Po activity ratio are indicated in order to provide an estimation of the dispersion of obtained ratios, as well as R² coefficients.

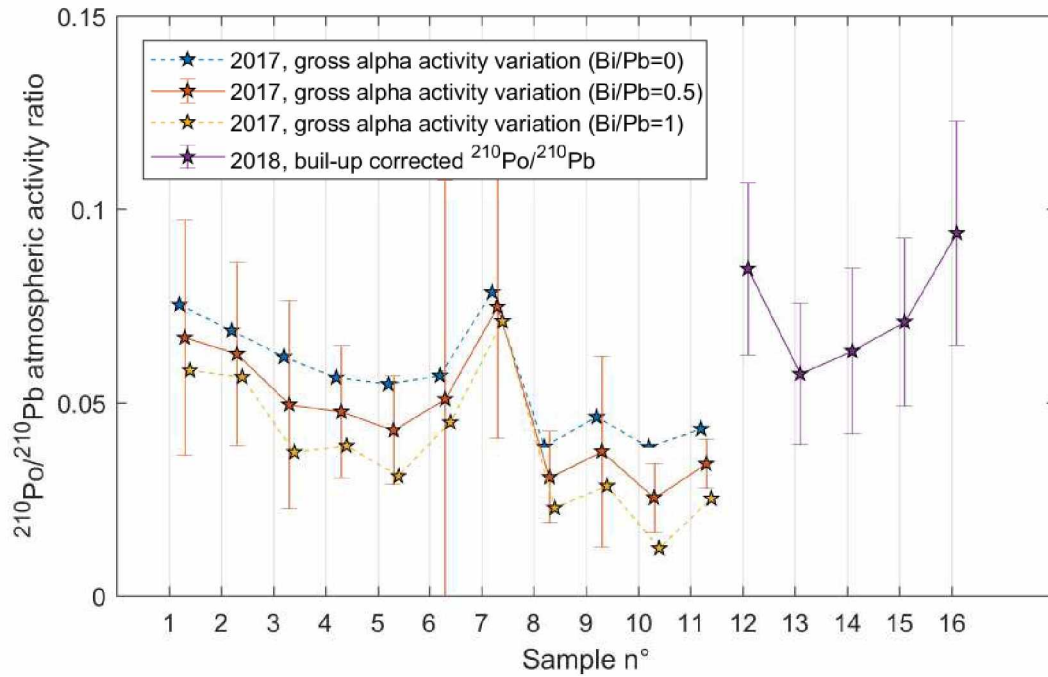


Figure 7: Comparison of atmospheric $^{210}\text{Po}/^{210}\text{Pb}$ activity ratios at sampling time retrieved using gross alpha activity variation between 5 and 50 days (2017 samples, samples n°1 to 11) and build-up corrected ^{210}Po activities divided by ^{210}Pb activities (2018 sample group, samples n°12 to 16). Ratios inferred from gross alpha activity variation (blue, red and yellow lines) are represented for different assumed values of the $^{210}\text{Bi}/^{210}\text{Pb}$ activity ratio (0, 0.5 and 1, respectively) and error bars ($k=2$) are propagated from uncertainties on 5 and 50-day gross alpha activities (error bars are only drawn on the red line). $^{210}\text{Po}/^{210}\text{Pb}$ activity ratio determined from corrected ^{210}Po activity and ^{210}Pb activity are plotted with error bars corresponding to the uncertainty ($k=2$) on ^{210}Po corrected activity value.

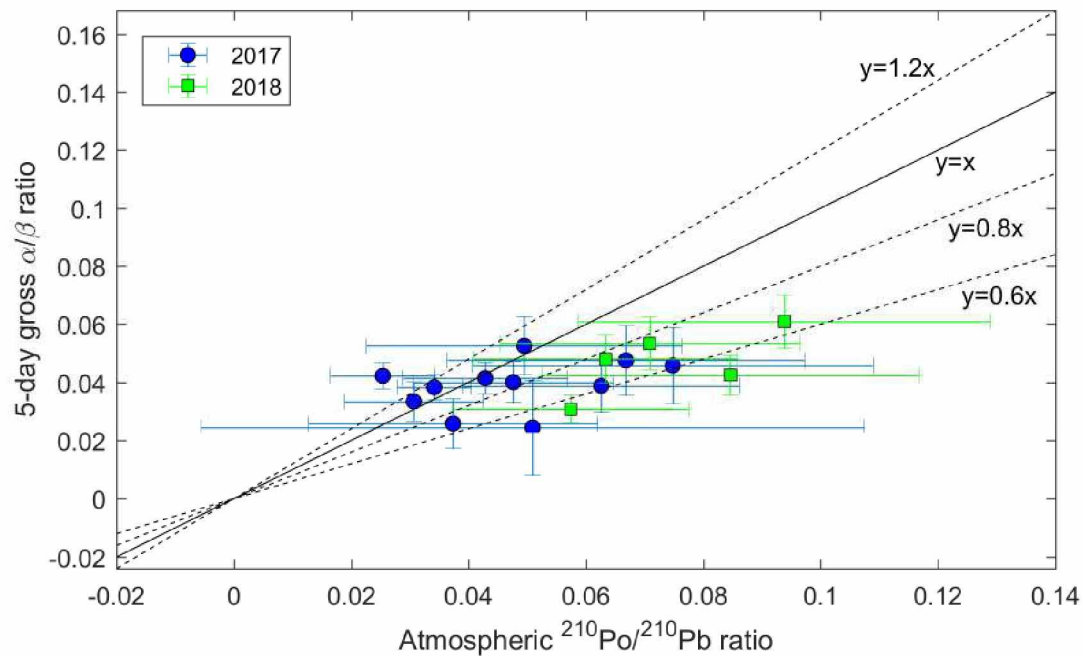


Figure 8: Gross alpha/beta activity ratio versus $^{210}\text{Po}/^{210}\text{Pb}$ activity ratios for 2017 samples (blue) and 2018 samples (green). For 2017 samples, $^{210}\text{Po}/^{210}\text{Pb}$ activity ratio is calculated using gross alpha activity variation between 5 and 50 days (see methods). For 2018 samples, $^{210}\text{Po}/^{210}\text{Pb}$ activity ratio is calculated using ^{210}Po and ^{210}Pb measurements with correction for ^{210}Po (see methods). All uncertainties have been propagated.